Article:

eprints@whiterose.ac.uk
https://eprints.whiterose.ac.uk/

Journal of Medical Robotics Research

https://www.worldscientific.com/worldscinet/jmrr

Journal of Medical Robotics Research

A Novel Mechanical Design of a Wearable Fingertip Haptic Device for Remote Meniscus Palpation

Samir Morad[*,§], Zainab Jaffer[†], Sanja Dogramadzi[‡]

[*]Department of Engineering, The University of East London
University Way, London, E16 2RD, UK

[†]Department of Life and Health Science
Aston University, Birmingham, B4 7ET, UK

[‡]Department of Automatic Control and Systems Engineering
The University of Sheffield, Sheffield, S1 3JD, UK

A pneumatic model of a fingertip haptic device (FHD) had been previously tested in virtual reality allowing the perception of different materials with a promising result. However, numerous drawbacks were noted in this design, including bulky size, less portability, and discomfort. In this paper, FHD is redesigned to provide haptic feedback for human meniscus palpation. A user study was performed to evaluate the effectiveness of the redesigned FHD. The study showed that the redesigned model could successfully provide a more evident perception of different stiffness levels but it compromised the comfort of the user when mounted on the finger for long periods.

Keywords: Surgical robotics, tele-operation, haptics, mechanical system, bolus materials.

—JMRR—

1. Introduction

Haptics is defined as touch feedback which can be divided into kinesthetic (force) and cutaneous (tactile) feedback. Within minimal invasive surgery (MIS), the goal of haptics is to allow "transparency" such that the surgeon feels like he/she is operating directly on the patient rather than on some remote body [1].

Currently, the majority of commercialized haptic devices, such as the Omega 3 haptic interface and the

NOTICE: Prior to using any material contained in this paper, the users are advised to consult with the individual paper author(s) regarding the material contained in this paper, including but not limited to, their specific design(s) and recommendation(s).

Phantom Premium 1.5, cannot be categorized as wearable. These haptic devices can produce a wide range of forces and are incredibly accurate. Since their base is anchored to the ground, they are also known as grounded interfaces. Exoskeletons are a type of haptic interface that is grounded to the body and were developed by researchers in the quest for more wearable haptic technologies [2].

Wearable haptic devices (WHDs), such as hand exoskeletons (HE), can increase mobility and replicate the operator's hand movements [3]. The combination of Cyberglove and CyberGras is an example of WHD which pulls the fingertips via cables to provide force feedback. Cables are also used in the glove to exert force on the fingers and measure the position of each finger [4]. In other WHDs, such as the DEXMO exoskeleton [5], rigid force transmission mechanisms attached to the hand are used to exert force on the fingers. Although DEXMO has high motion accuracy, one of its biggest drawbacks is that it can only produce binary haptic feedback. HEs can cover all or some of the fingers and can be made of rigid or soft materials. Some exoskeleton designs are bulky,

while others only cover the fingertips, which can be especially useful for tactile applications and controllable cutaneous feedback. A device with five vibro-tactile actuators, one for each user's fingertip, is an example of the use of vibration for haptic feedback [6]. Although most kinesthetic feedback is absent in wearable devices and only cutaneous stimuli are typically provided [7], it is still possible to make up for this shortcoming without significantly degrading performance [8].

One may think that haptic feedback is not very necessary, as visual feedback is sufficient to allow for successful surgeries. However, this lack of haptics prevents the identification of tissue consistency, which would enable the surgeon to discriminate between e.g. tissues with tumors and normal tissues [9] or detect arteries deeply rooted within tissues [10]. Furthermore, certain intricate and delicate procedures are involved in some surgeries. For example, within cardiac surgery, when suturing a coronary arterial anastomosis with a polypropylene suture, a surgeon is required to carefully puncture the artery using a needle, pull the suture through, form a knot and tighten it. The sense of touch is vital during this surgery as observations have shown that the excess forces applied by surgeons during robot-assisted minimal invasive surgery (RMIS) have led to delicate tissues being torn and the suture being broken. This presents the risk of irreversible injuries and may be detrimental to the patient [11].

In this paper we consider haptic feedback, more specifically cutaneous feedback, to orthopedic surgeons when discriminating between a healthy meniscus and a torn meniscus. The meniscus is a crescent-shaped cartilage that is found in the knee between the femoral condyle and tibial plateau. The primary role of a meniscus is to distribute the load across the tibiofemoral joint by increasing balance, thus reducing the resultant stress on the articular cartilage [12]. It plays a crucial role in load-bearing and shock absorption within the knee and acts as a secondary stabilizer for the joint [13]. The meniscus is mainly made up of water and type I collagen fibers [14]. The red zone of the meniscus (outer rim) is attached to the knee joint, the capsule is thick and convex in shape, whereas the white zone (inner edge) is unattached and concave in shape [15]. Meniscal tears are a very common orthopedic pathology [16]. The healthier parts of a meniscus feel stiffer than the torn parts of the collagen fibers breaking down and lending less support to the structure of the meniscus. For the treatment of a torn meniscus, surgeons need to identify the location of the tear and the border between the red and white zones. According to surgeons, the white zone is stiffer, and less elastic compared to the red zone, due to the absence of blood. This identification is crucial as it affects the decision on whether the torn meniscus needs to be repaired or excised.

Currently, orthopedic surgeons use a surgical tool during arthroscopy, which is an MIS procedure to repair a wide range of knee problems, to probe different locations on the meniscus and, using the visual feedback from a screen, differentiate between a healthy meniscus and a torn meniscus. During open surgeries, surgeons are able to get a lot more information as they can 'feel' the stiffness of the meniscus at different locations using their fingers. Another drawback with the lack of haptic feedback in arthroscopy is that new surgeons tend to apply much greater forces than required on the meniscus when being trained to perform these surgeries, which can cause further damage to the tissues. Hence, with sensory feedback, arthroscopic skills can be effectively passed on to trainees [17]. This study further mentioned that probing forces of greater than 8.5N on the meniscus should be avoided.

Previously, a pneumatic model of a fingertip haptic device (FHD) had been built and tested in virtual reality [18] by our group. This model was built using air as the medium to allow for changes in the levels of stiffness. The purpose of this device was to provide haptic feedback to the user, allowing them to perceive objects of different stiffness in virtual reality. Training new surgeons in virtual reality environments is a cost-effective substitute and provides a safe environment for trainees to develop their skills. The FHD was successful in mapping objects in virtual reality, however, due to its bulky size and discomfort upon mounting, it restricted the smooth movement of the surgeon's finger. Furthermore, due to its pneumatic design, the inflatable platform of the FHD does not provide consistent feedback to the user.

Hence, the purpose of the paper was to design a mechanical version FHD in an attempt of making it smaller, more compact, and more portable for its application in robotic surgery. The focus of the FHD2 is to map it to the varying levels of the stiffness of a human meniscus, rather than the bolus materials used with the previous design [19], for its use during orthopedic surgery.

2. Materials and Methods

2.1. *The construction of the mechanical FHD-FHD2*

The FHD is primarily designed to be used by surgeons during robotic surgery to allow them to 'feel' the difference between a healthy meniscus and a torn meniscus. For this reason, a common numerical parameter had to be determined that would allow the FHD2 to be mapped onto the meniscus. One of the properties that are used to define a meniscus is the aggregate modulus which is a measure of the stiffness of tissue at equilibrium [20]. The Young's modulus of the tissue can then be calculated using Eq. (1). A study by [21] tested the menisci of

different species at various locations. They measured the aggregate modulus of the anterior location of the human modulus to have a value of 160 ± 40 kPa, whereas that of the posterior and central locations are in the region of 100 ± 30 kPa. According to this study, the Poisson's ratio of the menisci at almost every location is zero. Applying Equation (1), where H_a is the aggregate modulus, E is Young's modulus and v is Poisson's ratio, Young's modulus will be exactly equal to the aggregate modulus.

$$H_a = E(1 - v)/[(1 + v)(1 - 2v)]. \tag{1}$$

Young's modulus and the spring constant are both a measure of stiffness, however, the spring constant relates to an object whereas Young's modulus relates to a material. Equation (2) displays a relationship between these two parameters, where k is the stiffness, A is the cross-sectional area, E is Young's modulus and l is the length.

$$k = \frac{AE}{l}. \tag{2}$$

2.2. Design and functionality of the FHD2

FHD2 consists of a foam layer attached to a spring layer via a foam base. These two layers of different stiffness objects are jointly corresponded to the meniscus (Fig. 1). To push the finger through the different levels of the FHD2, it was secured using a ribbon which was attached to the case and the shaft of the motor at the base of the FHD2 (Fig. 2). A rotary, servo motor (Turnigy MX-95E) was utilized in this case. When the motor shaft is rotated clockwise, the ribbon is pulled downwards, pushing the index finger into each level on the FHD2. When rotated in the opposite direction, the motor releases the tension in the ribbon, allowing the finger to move back to its original position.

The motor was programmed using an Arduino UNO board, thus moving it either only into level 1 (sponge), or through level 1 and into level 2 (springs) or through levels 1 and 2 and into level 3 (hard base).

For the first layer, a small section of foam material was selected to imitate the stiffness of the torn parts of a
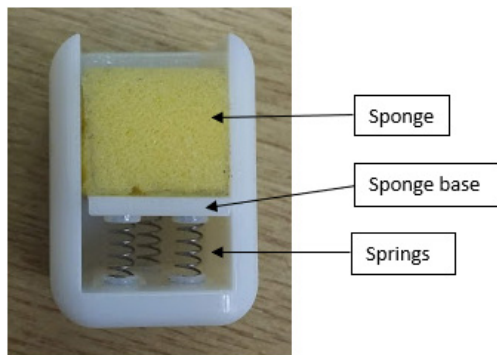

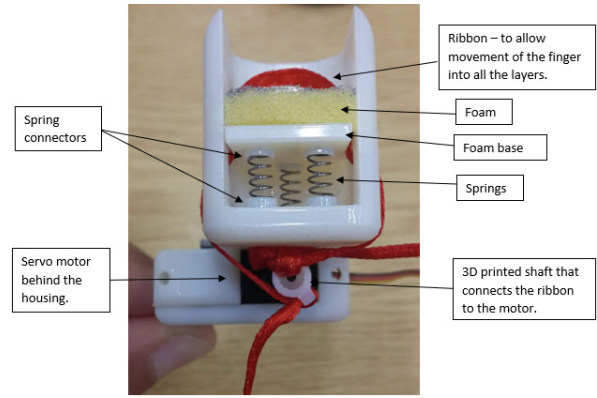**Fig. 1.** First assembled prototype of the mechanical design (FHD2).

Fig. 2. 3D printed and fully assembled model of the FHD2.

meniscus. During arthroscopic surgery, these cotton-like parts of the meniscus are excised to allow the stiff, healthy parts to be joined together.

The foam piece dimensions are 21.1 mm (length, l), 15.1 mm (width, w), and 15 mm (height, h) and its Young's modulus was determined before deciding on the springs to be used for the FHD2 model. A Young's modulus — density chart was used to determine Young's modulus of the foam piece [22]. Density, ρ, was calculated using Eq. (3), where W is weight, l is length, w is width, and h is the height of the sponge insert.

$$\begin{aligned} \text{Density} &= \frac{W}{l \times w \times h}, \\ \text{Density} &= \frac{0.09}{21.1 \times 15.1 \times 15}, \\ \text{Density} &= 1.88 \times 10^{-5} \text{gmm}^{-3} (0.01883 \text{Mgm}^{-3}). \end{aligned} \tag{3}$$

Based on M. F. Ashby's density chart [22] and using the calculated density of the foam piece, Young's modulus was recorded as 5×10^{-4} GPa.

Data collected during the analysis of the pneumatic model of a fingertip haptic device (FHD) [18] was used to select the springs for this prototype. From the analysis, it was concluded that the maximum force applied by the FHD on the fingertip was 7.01 N and the minimum force was 5.04 N. This maximum force was then used to calculate the approximate values for the required spring constants of the springs in this application, using the uncompressed and compressed lengths of the springs in this design.

To make the model as small as possible, the uncompressed length of the spring was chosen to be between 6 and 8 mm, and the compressed length to be approximately 2–4 mm. Equation (4) was used to calculate the spring constants using different combinations of compressed and uncompressed lengths. In this equation, F is the maximum force (7.01 N), k is the spring constant and e represents the compression, which is the difference between the uncompressed and compressed lengths.

$$F = ke. \tag{4}$$

S. Morad, Z. Jaffer & S. Dogramadzi

Spring constants of springs with different combinations of compressed and uncompressed lengths were calculated through a series of experiments (Table 1). Three kinds of compression springs with different spring constants but similar dimensions were considered for this application. These include 0.86 N/mm, 1.19 N/mm and 1.64 N/mm. Table 1 shows the calculated maximum forces required to fully compress all three kinds of springs. Since the design required three springs to be attached in parallel, the total spring constant was calculated. This provided a wider range of forces that could be experienced by the finger compared to the FHD [18].

Table 1. Spring constants of springs with different combinations of compressed and uncompressed lengths.

Uncompressed length (mm)	Compressed length (mm)	Compression (mm)	Total spring constant (N/mm)	Spring constant (Single spring) (N/mm)
6	2	4	1.75	0.58
6	3	3	2.34	0.78
6	4	2	3.51	1.17
8	2	6	1.17	0.39
8	3	5	1.40	0.47
8	4	4	1.75	0.58

Table 2. Maximum forces required to fully compress three different springs.

Spring constant (Single spring) (N/mm)	Total spring constant (N/mm)	Uncompressed length (mm)	Compressed length (mm)	Compression (mm)	Force (N)
0.86	2.58	8	2.60	5.40	13.9
1.19	3.57	8	3.00	5.00	17.9
1.64	4.92	8	3.40	4.60	22.6

All three springs were tested onto the printed model in Fig. 1. The last two options, i.e., 1.19 N/mm and 1.64 N/mm (Table 2) displayed the most distinct difference in the stiffness between the first and second levels (sponge and springs) of the FHD2, however, the forces required to push the finger into the springs were very high. The design for this model would require a motor to push the index finger of the user through each of the levels of varying stiffness (Fig. 1). A higher force would require a stronger and bulkier motor, which would compromise the compact size of the FHD2. Thus, springs with a spring constant of 0.86 N/mm were used as they required a lower force to push the finger into the device, and thus a smaller motor, while still displaying an evident difference between the two levels of stiffness on the FHD2.

2.3. *User study*

The aim of the study was to evaluate the effectiveness of the new mechanical design of the fingertip haptic device (FHD2) by comparing it to the pneumatic design of the fingertip haptic device (FHD).

Five volunteers, both males and females, in the age range 23-60 years, were asked to mount the FHD onto their fingertips. The device imitated five levels of stiffness through varying the levels of the soft platform inflation (Fig. 3).

A SingleTact pressure sensor was placed on the top of the variable compliance platform VCP to measure the forces experienced by the fingertip (Fig. 3(a)). The VCP was maintained at a constant position for all five levels to allow accurate measurements of force from the pressure sensor.

The subjects were then asked to mount the FHD2 onto their fingertip. A qualitative and quantitative analysis was used during this study. The qualitative questions asked the subjects to arrange the levels of stiffness experienced in both devices in order of softness and to compare the haptic feedback provided by both the
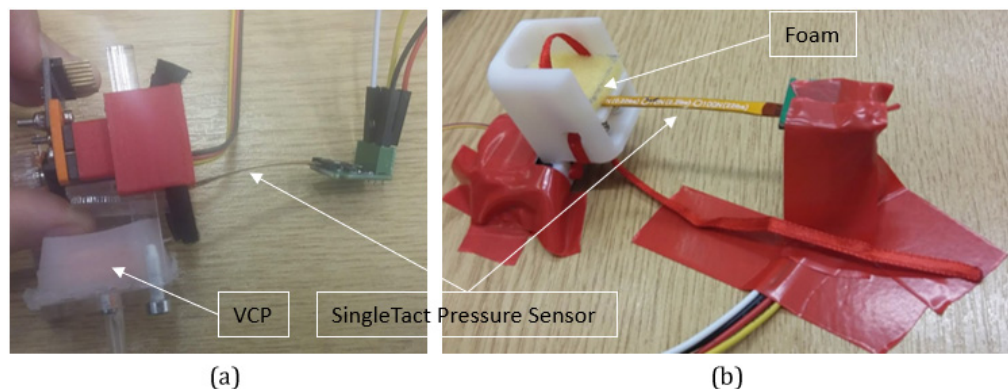

Fig. 3. Attachment of the SingleTact sensor for the user study (a) to FHD, (b) to FHD2.

devices. The results from these questions were used to analyze which design of the FHD is more effective in providing haptic feedback. The quantitative data obtained through the pressure sensor was also analyzed and compared to the qualitative results to certify them. This device imitated three levels of stiffness. The forces experienced by the fingertip were also measured, using the same pressure sensor. The setup of this device for the user study can be seen in Fig. 3(b).

3. Results and Discussion

Figures 4 and 5 represent the forces experienced by the finger at different levels in FHD (pneumatic model) and FHD2 (mechanical model) respectively. The figures show that the FHD2 allows subjects to experience a range of forces from 4.9 N to 8.6 N, when compared to FHD, where the forces on the index finger range between 5.3 N and 7.5 N. This is possibly the reason why four out of the five subjects in this user study mentioned that the FHD2

provided a more distinct perception of the changes in the level of softness compared to the FHD.

Interestingly, all five subjects were successful in correctly arranging the different levels of stiffness on the devices with the correct order of softness. For FHD, the more inflated the device was, the harder stiffness level was perceived (1 ml of air represented the softest level and 5 ml of air represented the hardest level). For FHD2, compression into the sponge represented the softest level and compression halfway into the springs represented the hardest level.

The difference in the forces experienced by the subjects between the different levels in FHD2 (Fig. 5) allows a more distinct perception of changes in the level of softness. In particular, users commented that a very big difference was felt between levels 2 and 3. This is also evident from the force measurements as the two levels had a difference of about 2 N.

Two out of the five subjects rated the level of comfort of both devices as moderate. However, three of them preferred the comfort level in FHD, commenting that the ribbon in FHD2 applied high pressures on the top of the finger. Furthermore, three out of five subjects also mentioned that the feedback from FHD2 was too strong, while all of them thought that the feedback from FHD was sufficient. It seems that the users preferred a more subtle feedback like in the pneumatic model. Also, due to the small width of the ribbon, the pressure was concentrated on a small area at the top of the index finger. This could also possibly be a source of discomfort/cause the feedback to be too strong.

Upon analysis of the new model and the feedback received by the subjects, it was obvious that even though the device was effective in imitating at least two levels of stiffness of a meniscus, it is quite different from being able to feel the tissue using the human fingers. The meniscus is a tissue, and it is assumed that it would feel quite different compared to sponges and springs. The main point is that even if it does feel different, surgeons can be trained to learn the difference, if any. However, this difference can be made evident to surgeons during training programs, so that they are able to relate each level on the FHD to the meniscus. For example, the softest level (foam) corresponds to the torn parts of a meniscus, and so on.
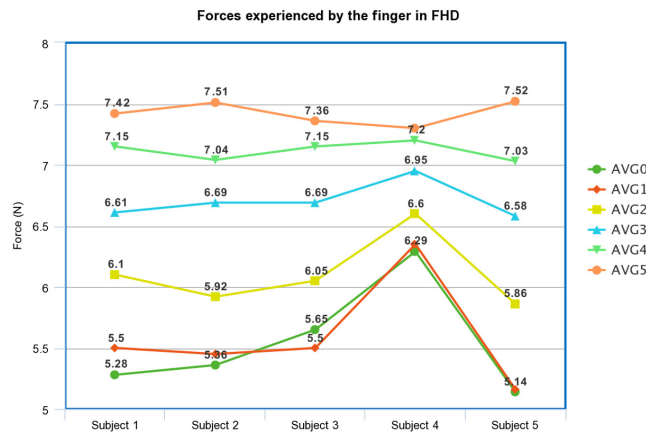

Fig. 4. Graph displaying the forces experienced by the finger at different levels in FHD.
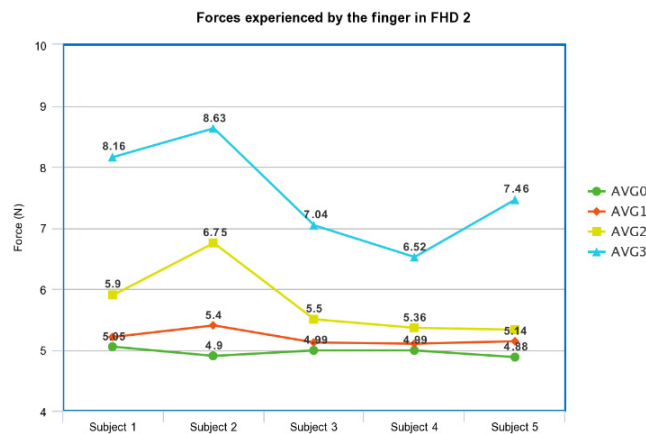
4. Conclusion

In this study, a mechanical version (FHD2) of a previously designed pneumatic FHD was developed to increase its application from virtual reality to physical materials, and eventually to a human meniscus application. A user study was conducted to compare the effectiveness of the two FHD designs (pneumatic and mechanical) to evaluate the redesigned FHD model (FHD2). The study found that FHD

Fig. 5. Graph displaying the forces experienced by the finger at different levels in FHD2.

was more comfortable when mounted on the finger than FHD2. However, FHD2 enabled a more apparent change in stiffness levels than FHD. Also, FHD2 was designed to be smaller and more portable after eliminating the pneumatic system used in FHD.

The group plans to increase the comfort of using the FHD2 by controlling the feedback from the device to be within a comfortable range.

References

1. A. M. Okamura, Haptic feedback in robot-assisted minimally invasive surgery, *Curr. Opin. Urol.* **19**(1) (2009) 102–107.

2. S. J. Biggs and M. A. Srinivasan, Haptic interfaces, in *Handbook of Virtual Environments* (Lawrence Erlbaum, NJ, 2002), pp. 93–116.

3. O. A. J. van der Meijden and M. P. Schijven, The value of haptic feedback in conventional and robot-assisted minimal invasive surgery and virtual reality training: a current review. *Surg. Endosc.* **23**(6) (2009) 1180–1190.

4. Y. Park, I. Jo, J. Bae, Development of a dual-cable hand exoskeleton system for virtual reality, in *Proc IEEE/RSJ Int. Conf. Intelligent Robots and Systems (IROS)* (South Korea, Daejeon, (2016), pp. 1019–1024.

5. X. Gu, Y. Zhang, W. Sun, Y. Bian, D. Zhou and P. O. Kristensson, Dexmo: An inexpensive and lightweight mechanical exoskeleton for motion capture and force feedback in VR, in *Proc CHI Conf. Human Factors in Computing Systems* (2016), pp. 1991–1995.

6. A. T. Maereg, A. Nagar, D. Reid, and E. L. Secco, Wearable vibrotactile haptic device for stiffness discrimination during virtual interactions. *Front. Robot. AI.* **4**(42) (2017).

7. D. Prattichizzo, F. Chinello, C. Pacchierotti and M. Malvezzi, Towards wearability in fingertip haptics: a 3-dof wearable device for cutaneous force feedback, *IEEE Trans. Haptics* **6**(4) (2013) 506–516.

8. C. Pacchierotti, A. Tirmizi and D. Prattichizzo, Improving transparency in teleoperation by means of cutaneous tactile force feedback, *ACM Trans. Appl. Percept.* **11**(1) (2014) pp. 4–16.

9. G. Tholey, J. P. Desai and A. E. Castellanos, Force feedback plays a significant role in minimally invasive surgery: results and analysis, *Annal. Surg.* **241**(1) (2005) 102–109.

10. A. A. Mehrizi, S. Najarian, M. Moini, J. Dargahi and R. Ahmadi, A novel method in exploration of arteries inside a tissue and assessment of the arteries by computational approach, *IEEE/ASME Int. Conf. Advanced Intelligent Mechatronics*, Montreal, ON (2010), pp. 932–936.

11. A. M. Okamura, Methods for haptic feedback in teleoperated robot-assisted surgery, *Ind. Robot, Int. J.* **31**(6) (2004) 499-508.

12. A. J. Fox, F. Wanivenhaus, A. J. Burge, R. F. Warren and S. A. Rodeo, The human meniscus: A review of anatomy, function, injury, and advances in treatment, *Clin. Anatomy* **28**(2) (2015) 269–287.

13. I. D. McDermott, S. D. Masouros and A. A. Amis, Biomechanics of the menisci of the knee, *Curr. Orthopaedics* **22** (2008) 193-201.

14. J. Herwig, E. Egner and E. Buddecke, Chemical changes of human knee joint menisci in various stages of degeneration, *Ann. Rheumatic Diseases* **43**(4) (1984) 635–640.

15. E. Rath and J. C. Richmond, The menisci: basic science and advances in treatment, *Brit. J. Sports Med.* **34** (2000) 252–257.

16. S. C. Mordecai, N. Al-Hadithy, H. E. Ware and C. M. Gupte, Treatment of meniscal tears: An evidence-based approach, *World J Orthop.* **5**(3) (2014) 233–241.

17. G. J. M. Tuijthof, T. Horeman, M. U. Schafroth, L. Blankevoort and G. M. M. J. Kerkhoffs, Probing forces of menisci: what levels are safe for arthroscopic surgery, *Knee Surg. Sports Trauma. Arthroscopy* **19**(2) (2011) 248–254.

18. A. Tzemanaki, G. A. Al, C. Melhuish and S. Dogramadzi, Design of a wearable fingertip haptic device for remote palpation: Characterisation and interface with a virtual environment, *Front. Robot. AI* **5**(62) (2018) 6633–6655.

19. S. Morad, Z. Jaffer and S. Dogramadzi, Design of a wearable fingertip haptic device: investigating materials of varying stiffness for mapping the variable compliance platform, *J. Med. Robot. Res.* **6**(03n04), 2150005 (2021).

20. J. M. Mansour, Biomechanics of cartilage, *Kinesiology: Mech. Pathomech. Human Movement* **2** (2003) 66–79.

21. M. A. Sweigart, C. F. Zhu, D. M. Burt, P. D. deHoll, C. M. Agrawal, T. O. Clanton and K. A. Athanasiou, Intraspecies and Interspecies Comparison of the Compressive Properties of the Medial Meniscus, *Ann. Biomed. Eng.* **32**(11) (2004) 1569–1579.

22. M. F. Ashby, *Materials Selection in Mechanical Design*, 3rd edn. (Butterworth-Heinemann, Oxford, 2005).

Samir Morad received the BEng degree in medical engineering from Queen Mary College, University of London, London, UK, in 2010 and the MSc. degree in biomedical engineering from Imperial College London, London, UK, in 2011, and PhD. degree in medical robotics from Imperial College London, London, UK, in 2015. He is currently a lecturer in mechanical engineering and the leader of the biomedical engineering programme at the department of architecture, computing and engineering at the University of East London. From 2016 to 2019 Dr. Morad was a teaching associate in biomedical engineering at the department of life and health science at Aston University. From 2015 to 2016 Dr. Morad was a Research Fellow in medical robotics at Bristol Robotics Laboratory. His research interest includes the development of robot assisted flexible surgical intervention, 3D reconstruction and FEA analysis of human tissues.

Zainab Jaffer received her MEng degree in Biomedical Engineering from Aston University, UK. From 2018 to 2019, Zainab was at Bristol Robotics Laboratory, as an internship, as part of her Meng project, working on SMARTsurg Project.

Sanja Dogramadzi received her MEng degree in Mechatronics, robotics, and automation Engineering from the University of Belgrade, Serbia, and her Ph.D. degree robotic endoscopy from the University of Newcastle upon Tyne, UK. She is currently Professor of Medical Robotics and Intelligent Healthcare Technologies at the Department of Automatic Control and Systems Engineering at the University of Sheffield. From 2002 to 2006, Prof Dogramadzi was at the University of Leeds, as Research Fellow, and from 2006 to 2020 she was at Bristol Robotics Laboratory, University of the West of England, as Senior lecturer /Associate/Full Professor. Sanja Dogramadzi is the author of over 127 publications. Her research interests include design and control of surgical robots for minimally invasive fracture surgery and robot-assisted MIS, rehabilitation robots, physical assistance robots and safe and ethical human-robot interaction. She has led and coordinated many research projects funded by UK councils, Innovate UK, NIHR and European Commission.